Cu(I)–O2 Oxidation Reactions in a Fluorinated All–O–Donor Ligand Environment

Journal:	*Dalton Transactions*
Manuscript ID	DT-PER-12-2018-005028.R1
Article Type:	Perspective
Date Submitted by the Author:	15-Feb-2019
Complete List of Authors:	Brazeau, Sarah; Boston University, Chemistry Doerrer, Linda; Boston University, Chemistry Department

Prof. Linda H. Doerrer

Boston University

Chemistry Department

590 Commonwealth Ave., SCI 383

Boston, MA 02215

(617) 358-4335

15 February 2019

Dear Professor Holder,

Please find attached our manuscript entitled "Cu(I)-O$_2$ Oxidation Reactions in a Fluorinated All-O-Donor Ligand Environment" which we are submitting for publication consideration as an invited perspective article in *Dalton Transactions* in honor of Professor Geoff Cloke.

We are responding to the reviewers' helpful and detailed comments as described below.

Reviewer 1:

1. Introduction, first paragraph. "Oxidation reactions can be either oxidase, monooxygenase, or dioxygenase". These are rather enzyme types/enzymatic mechanisms; the author should define them and comment on the differences.

   A brief expansion in the text to clarify has been added as well as one dioxygenase enzyme to Scheme 1.

2. What is "E" in Scheme 3?

   "E = Si or Al" has been added to the caption of Scheme 3 for clarification.

3. It is not immediately obvious what is the starting material in Scheme 7 – it took me a few moments to understand that it is CuMes. Can the layout of the scheme be improved to make it more clear what reagents lead to what outcomes? Furthermore, the subsequent discussion in the paper highlights differences between compounds which have some degree of structural similarity, yet differing from one another in other aspects. For example, when the author describes the interaction between Cu(I) complexes and O2, it is hypothesized (for compounds 4 and 7) that less K---O/F lead to "…diminished ability to generate a stable {Cun-O2} species…". Yet, the relevant schemes (Scheme 5 and 7) only demonstrate similarity between the compounds, not differences. In my view, there needs to be one big scheme/table/figure in the manuscript in which there would "one-to-one" assignment of the compounds with their respective numbers so the reader could easily link reactivity differences with the structural ones.

   Scheme 7 (now scheme 6) has been expanded substantially to make the nature of the reactions and the compound numbering clear.

4. The authors describe encapsulation of the potassium ions by the alkoxide ligands' fluorines; while the solid-state information on the strength of such interaction can be obtained from the structural studies, the nature of K--F interaction in solution is deduced primarily from the conductivity studies. I am curious whether it could be possible to use ^{19}F NMR spectroscopy to estimate K---F interaction in solution?

For 1-6, ^{19}F NMR spectra are nearly identical between encapsulated and unencapsulated complexes. In light of this suggestion, a sentence has been added to the conclusions to address future variable temperature ^{19}F NMR experiments that further explore K···F/O interactions. We have a manuscript in preparation on some Sn(IV) compounds that do exhibit temperature- dependent fluxionality.

5. Scheme 5 should have compounds #s in it: it would be easier to follow the text this way

Scheme 5 includes non-Cu examples of fluorinated O-donor complexes, as background material from our group, which are not discussed significantly in the text. Only the Cu-containing complexes have been numbered, and Scheme 6 (previously scheme 7) has been revised to make their identities clearer.

6. There are several clear advantages to using fluorinated ligands in catalysis in general, and the oxidation catalysis in particular. The steric/electronic argument (fluorination reduces basicity, prevents bridging, and forms mononuclear species) is very much valid and is clearly presented in the paper. The authors also talk about fluorine atoms providing ligands to the intercalated alkali metals, which contributes to the overall stability of the complexes by creating less charge separation. There is one point that, in my view, could be further elaborated, and that is the stability/robustness of F-substituted hydrocarbons under oxidizing conditions – this consideration, I think, is particularly relevant to the application discussed here. This point is addressed later in the manuscript, but not in initial discussion on the advantages of the fluorinated ligands.

A sentence has been added to the introduction to address this additional advantage of fluorinated ligands.

7. What is the structure of the DFT-proposed asymmetric trimer (asT)? Scheme 10 describes the overall transformation with all possible intermediates, including the ones which are not observed ("M"). However, "asT" does not appear there.

Now Scheme 9, this has been expanded in order to incorporate the asymmetric trimer.

Reviewer 2:

1. In discussing tyrosinase activity it might be appropriate to cite a few papers from the group of F. Tuczek. That group has made many pioneering contribution to the field of tyrosinase chemistry.

   To account for the ongoing area of research in tyrosinase models, we now cite multiple papers and a review by Tuczek, as well as papers from other relevant groups, including Casella, Herres-Pawlis, Stack, and Lumb.

2. In many of the schemes the authors have used "normal" formulae to describe many compounds. The manuscript will become much more readable if the authors use appropriate Chemdraw figures in those schemes instead of normal formulae.

   The substantial revisions to Scheme 6 (previously scheme 7) should address this point.

Thank you for considering our paper.
Sincerely,
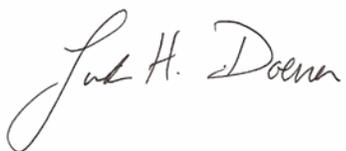
Dalton Transactions

ARTICLE

Cu(I)-O$_2$ Oxidation Reactions in a Fluorinated All-O-Donor Ligand Environment

Sarah E.N. Brazeau and Linda H. Doerrer*

Investigation of Cu-O$_2$ oxidation reactivity is important in biological and anthropogenic chemistry. Zeolites are one of the most promising Cu/O based oxidation catalysts for development of industrial-scale CH$_4$ to CH$_3$OH conversion. Their oxidation mechanisms are not well understood, however, highlighting the importance of the investigation of molecular Cu(I)-O$_2$ reactivity with O-donor complexes. Herein, we give an overview of the synthesis, structural properties, and O$_2$ reactivity of three different series of O-donor fluorinated Cu(I) alkoxides: K[Cu(OR)$_2$], [(Ph$_3$P)Cu(μ-OR)$_2$Cu(PPh$_3$)], and K[(R$_3$P)Cu(pin^F)], in which OR= fluorinated monodentate alkoxide ligands and pin^F= perfluoropinacolate. This breadth allowed for the exploration of the influence of the denticity of the ligand, coordination number, the presence of phosphine, and K···F/O interactions on their O$_2$ reactivity. K···F/O interactions were required to activate O$_2$ in the monodentate-ligand-only family, whereas these connections did not affect O$_2$ activation in the bidentate complexes, potentially due to the presence of phosphine. Both families formed trisanionic, trinuclear cores of the form {Cu$_3$(μ_3-O)$_2$}$^{3-}$. Intramolecular and intermolecular substrate oxidation were also explored and found to be influenced by ligand coordination. Namely, {Cu$_3$(μ_3-O)$_2$}^{3} from K[Cu(OR)$_2$] could perform both monooxygenase reactivity and oxidase catalysis, whereas those from K[(R$_3$P)Cu(pin^F)] could only perform oxidase catalysis.

Introduction

Catalytic oxidation reactions are fundamental processes on earth – both in biology and in synthetic chemical conversions. A detailed understanding of their properties and iterative improvements in performance are important goals for fundamental and applied reasons. Oxidation reactions can be either oxidase, monooxygenase, or dioxygenase, as shown in Scheme 1. In oxidase reactions the substrate is oxidized without the introduction of atoms from O$_2$ which are reduced and form H$_2$O. In monooxygenase and dioxygenase reactions, on the other hand, one or two O atoms from O$_2$, respectively, are incorporated into the substrate. In designing new oxidants, enzymes such as ascorbate oxidase, particulate methane monooxygenase (pMMO), dually reactive tyrosinase,[1] quercetin 2,3-dioxygenase[2] and others have served as inspirations because these enzymes catalyze desirable transformations under ambient conditions (Scheme 1).[3, 4] In particular, tyrosinase reactivity has been widely studied via model complexes and is an ongoing area of interest.[5-12] A common trait among this enzyme group is a Cu active site that activates O$_2$ to effect intermolecular oxidation reactions.[3] Of particular interest is C-H bond functionalization, such as the oxidation of CH$_4$ to CH$_3$OH by pMMO. To better understand these transformations in Cu enzymes, a large array of Cu(I) model complexes that reduce O$_2$ have been prepared to explore both

formation of reactive {Cu$_n$-O$_2$} intermediates performing (sub)stoichiometric and/or catalytic substrate oxidation.[13-15] The coordination spheres of these model complexes are dominated by N-donor ligands, due to the prominence of imidazole donors in enzymes and their ease of synthetic modifications. While investigation of these complexes has led to an increasingly sophisticated understanding of how ligand environments influence intermediate formation and reactivity, none of these models perform usefully on an industrial scale.

Zeolites have shown considerable promise as industrial oxidation catalysts, having been used as catalysts by petrochemical companies since the 1960s.[16] Rather than N-donor ligands, all zeolites bear anionic aluminosilicate O-donor frameworks, as shown in Scheme 2, and can be loaded with a variety of metal cations. By tuning zeolite properties, these materials can be adapted to a number of industrial refining processes, finding particular success as a fluid catalytic cracking (FCC) catalyst, which produces primarily gasoline from crude oils.[17] Zeolites have also been examined for other reactions. Two of the most studied for oxidation reactions are Zeolite Socony Mobil–5 (ZSM-5) with MFI framework, and mordenite (MOR). Both frameworks have similar Cu coordination environments that are proposed sites for reaction with O$_2$, with nearly identical structural properties.[16, 18]

Notably, activated Fe and Cu zeolites have been shown to catalytically oxidize substrates, including the most difficult one, CH$_4$, first achieved by Fe/O ZSM-5,[19] and later by Cu/O ZSM-5.[20] While Fe/O ZSM-5 is a stronger oxidant of CH$_4$ compared to Cu/O ZSM-5, Fe/O ZSM-5 requires N$_2$O for activation, whereas Cu/O ZSM-5 can be activated by either N$_2$O or O$_2$, making it more fit for industrial

Department of Chemistry, Boston University, Boston, Massachusetts 02215, USA.
*E-mail: doerrer@bu.edu; Tel: +1 617 358 4335*
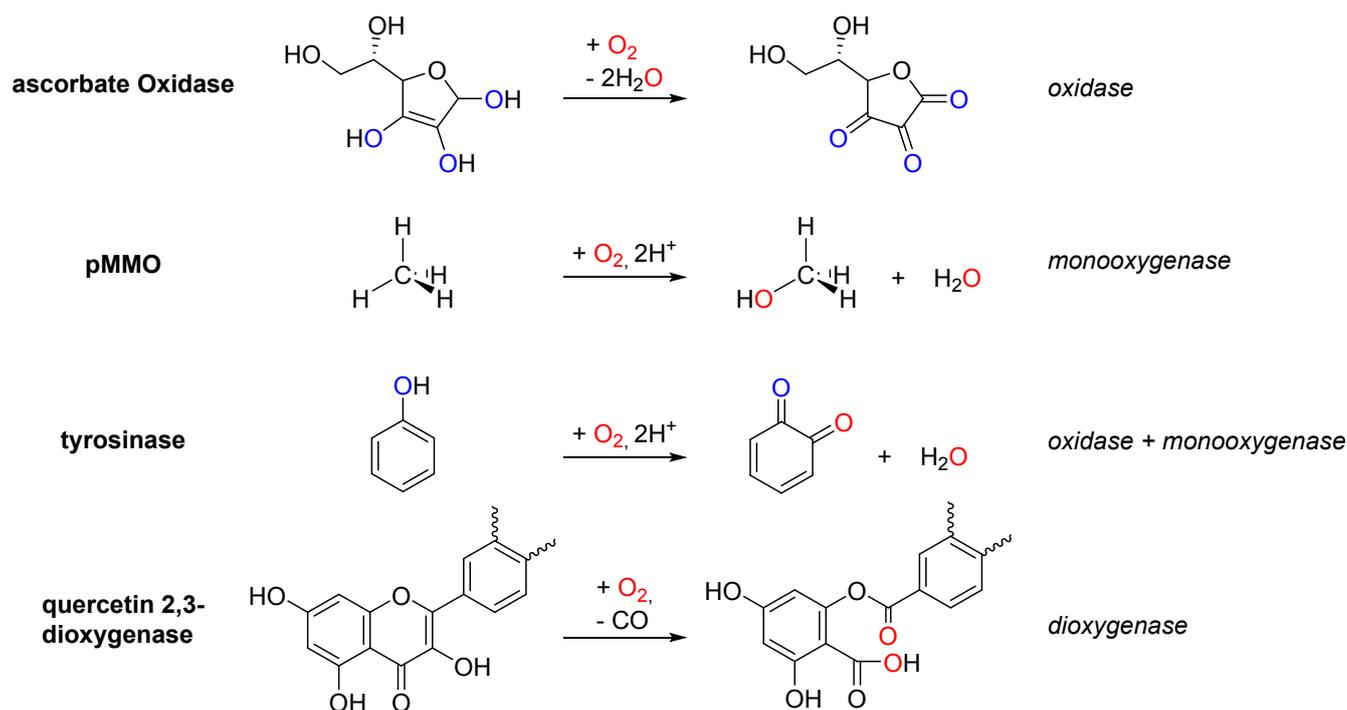
**Scheme 1.** Oxidation processes catalyzed by representative enzymes.
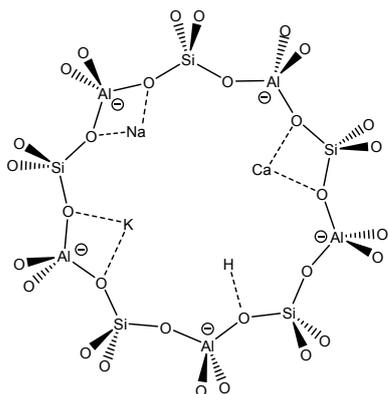
Scheme 2. Generic zeolite pore with anionic aluminosilicate framework and examples of metal cations.

application.[16] Additionally, Cu/O ZSM-5 requires a temperature of only 150 °C to activate CH_4, has a selectivity greater than 98%,[20] and has well-understood active site(s).[16, 18, 21, 22] In Cu/O ZSM-5, the mechanism of formation of the active site was fully characterized. As shown in Scheme 3, each Cu site is coordinated bidentate to the O-donor framework, and when exposed to O_2, forms a μ-η^2:η^2 peroxo-bridged dicopper intermediate, which rearranges to $\{Cu_2O\}^{2+}$.[21, 22] Similarly, Cu-MOR also catalyzes CH_4 to CH_3OH oxidation, bearing two related $\{Cu_2O\}^{2+}$ active sites with the same core structure.[18] More recently, Cu/O zeolites that oxidize CH_4 with $[Cu_3O_3]^{2+}$ have been investigated in ZSM-5 and MOR.[23-25]

To develop molecular oxidants based on zeolite active sites, the use of O-donor ligands is necessary. Hydrogenated O-donor ligands are
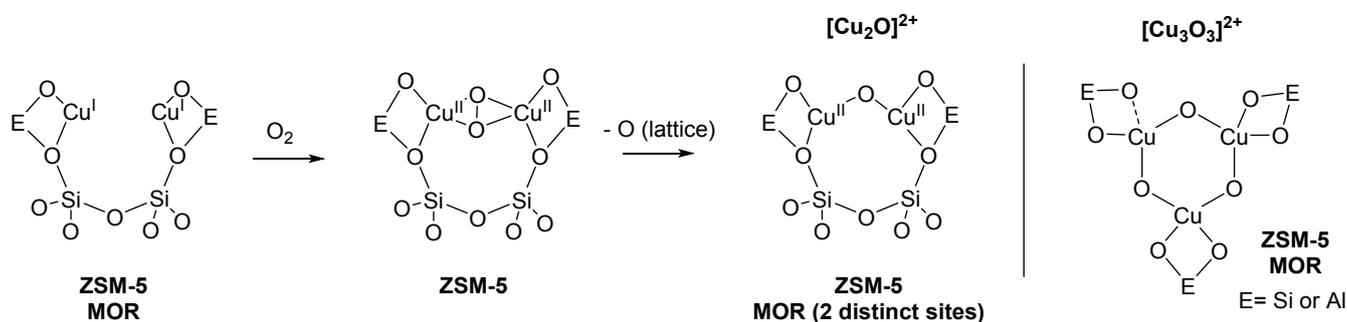
Scheme 3. Proposed reactive species in Cu/O zeolites ZSM-5 and MOR, based on *Chem. Rev.* **2018**, *118*, 2718, *Nat. Comm.* **2015**, *6*, 7546, and *J. Catal.* **2016**, *338*, 305.
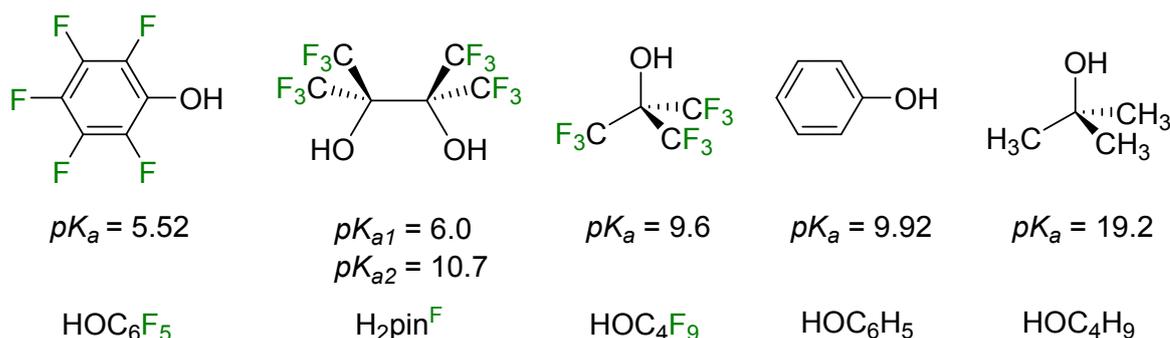
Scheme 4. Decreasing alcohol pK_a values with increasing fluorine content.

challenging to work with primarily due to oxidative ligand degradation but also due to high pK_a values, which increase the degree of bridging, possible polymerization, and reduced open coordination sites.[26]

Additionally, higher spin states are known to promote oxidation chemistry, including high-spin Co(II),[27] high spin Fe(III),[28] and intermediate spin Ru(IV).[29] Fluoride is known to promote high oxidation states when bound to metal centers including $[Cu^{IV}F_6]^{2-}$, $[Co^{IV}F_6]^{2-}$, $[Rh^{VI}F_6]$, and $[Re^{VII}F_7]$.[30] When ligands are highly fluorinated, pK_a values are generally decreased, as shown in Scheme 4, due to increased stabilization of the conjugate base upon fluorination.[31] Carbon-fluorine bonds are robust to most oxidation conditions, making perfluorinated ligands well suited for catalytic reactivity with O_2. The decreased basicity of fluorinated ligands also results in lower propensity for bridging under analogous conditions.[32, 33] In fluorinated alkoxide complexes, fluorine can often interact reversibly with Lewis acidic alkali metal cations, lending to greater complex stability.[34-40]

Our research group has successfully demonstrated the combined benefits of fluorination and O-donor ligands, including stabilizing complexes with high formal oxidation states[41, 42] as well as high spin states.[43] For example, a monomeric organocuprate complex with Cu^{III}, $\{K(18C6)\}[Cu^{III}(OC(C_6H_4)(CF_3)_2)_2]$, was found to be stable at room temperature, with the partially fluorinated α-cumyl alkoxide ligand backbone.[41] We have also observed high-spin square-planar behavior with $[Fe^{II}(pin^F)_2]^{2-}$ and $[Co^{II}(pin^F)_2]^{2-}$, with the

perfluoropinacolate (pin^F) ligand, shown in Scheme 4.[43] More recently, a square-planar $[Co^{III}(pin^F)_2]^-$ complex was isolated, with an intermediate $S = 1$ spin state and exceptionally large zero-field splitting.[42]

Fluorinated Alkoxide Complexes

There now exists a large number of complexes with fluorinated alkoxide ligands, and some representative complexes can be seen in Scheme 5. These include primarily mononuclear, homoleptic aryloxide and alkoxide 3*d* metal complexes. For example, four-coordinate monodentate high spin complexes with either OC_6F_5 or $3,5-OC_6H_3(CF_3)_2$ ligand environments were synthesized with Co(II),[32] Ni(II),[44] Cu(II),[32] and Zn(II),[45] and a five-coordinate Fe(II) complex.[46] The perfluoro-*t*-butoxide (OC_4F_9) ligand was also employed, supporting unusual three-coordinate complexes with Fe(II), Co(II), and Cu(II).[47] A series of homoleptic Zn(II) complexes was also prepared with fluorinated aryloxides and the α-cumyl alkoxide, $OCPhMe^F_2$, with the coordination number of Zn dependent on ligand steric bulk.[45] Several dimeric species have been prepared with 3*d* metals as well.[32, 45, 46] We have also used the bidentate pin^F ligand to prepare several room-temperature and air stable complexes. Divalent complexes with the form $[M(pin^F)_2]^{2-}$ were initially reported by C.J. Willis and co-workers with M = Mn, Ni, Cu and Zn, but characterized only by elemental analysis and magnetic susceptibility.[48] Our group characterized these species more thoroughly, and prepared several new complexes as well.[42, 43, 49]
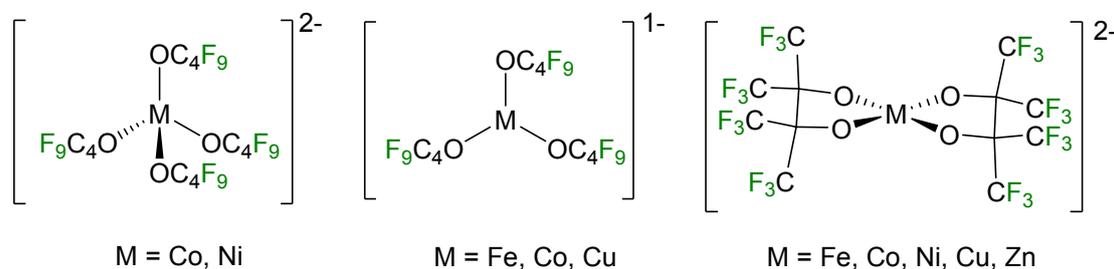
Scheme 5. Selection of O-donor fluorinated complexes synthesized by our research group.

We have since applied our unique ligand systems to investigate the efficacy of all-O-donor molecular systems in intermolecular oxidation. As mentioned above, investigations in this area have been dominated by N-donor ligands,[13-15] structurally, spectroscopically, and (sometimes) functionally mimicking those from nature and leading to a greater understanding of their mechanisms. To date, however, none of these systems have been adapted commercially. The ability of O-donor zeolites to catalyze conversion of CH_4 to CH_3OH highlights the necessity of a deeper exploration of O-donor Cu(I) complexes and their reactivity with O_2. While there are some examples of mixed N/O-donor scaffolds,[50-60] our work constitutes the only fully O-donor ligand environment in molecular Cu-O_2 chemistry.
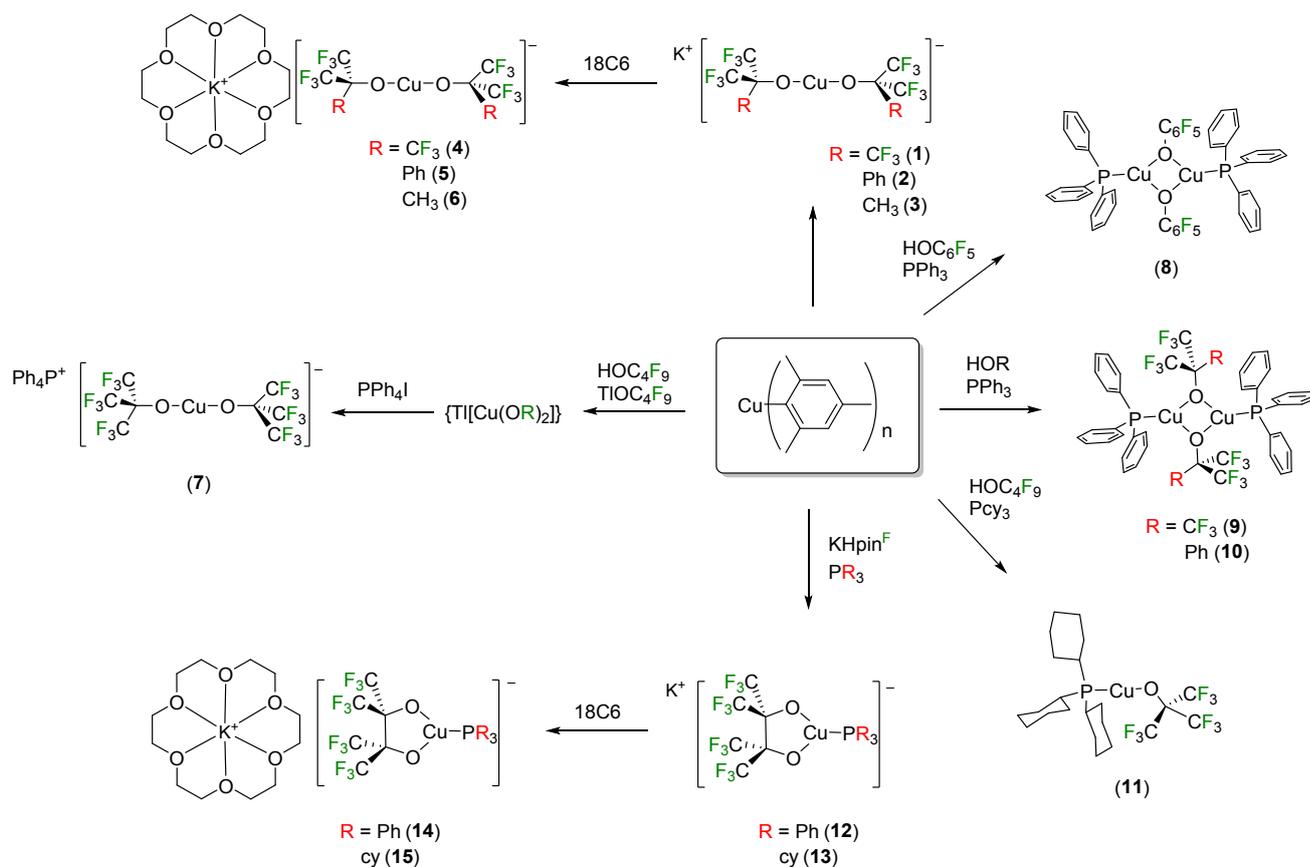
Scheme 6. Syntheses of Cu(I) O-donor complexes.

## Application of all O-donor ligand environment for Cu-O₂ Reactivity

Cu(I) Complexes with O-donor Ligands

Cu(I) O-donor fluorinated complexes were synthesized in an anoxic, anhydrous environment. To date, there are three different complex families (Scheme 6): linear Cu(I) bis-alkoxide complexes, [Cu(OR)$_2$]$^-$ (OR= OC$_4$F$_9$ (**1, 4, 7**); OCPhMe$^F_2$ (**2, 5**); OCMeMe$^F_2$ (**3, 6**)),[61] the dimeric [(Ph$_3$P)Cu(u-OR)$_2$Cu(PPh$_3$)] (OR= OC$_6$F$_5$ (**8**), OC$_4$F$_9$ (**9**), OCPhMe$^F_2$ (**10**),[62] with formation of [(cy$_3$P)Cu(OC$_4$F$_9$)] (**11**) in the presence of a bulkier phosphine,[62] and three coordinate [(R$_3$P)Cu(pin^F)]$^-$(PR$_3$= PPh$_3$, Pcy$_3$) (**12 - 15**).[63] All are synthesized in a similar fashion, shown in Scheme 6, first using alcoholysis with {Cu^I(mes)}$_n$,[64, 65] followed by addition of alkoxide salts and neutral ligands where necessary.

Structural characterization of **1-3** revealed the linear coordination one would expect, in addition to extensive interactions of unencapsulated K$^+$ ions with the ligand O and F atoms.[61] The K$^+$ counter cations were encapsulated with 18C6 (**4-6**, respectively) for structural comparison. Comparing **1**, shown in Scheme 7, to **4** the number of K···F/O interactions decreases from ten to one in the solid state.[61] A PPh$_4^+$ complex (**7**) was also synthesized via in-situ generated Tl[Cu(OC$_4$F$_9$)$_2$]. Complexes **1-7** are all linear in the O-Cu-O angle, with the number of K···F/O interactions dependent on the degree of K$^+$ encapsulation.[61] Additionally, **2** also contains two cuprophilic interactions[66-73] in the solid state, which are attributed to K···F/O interactions linking adjacent complexes together.[61] These low-coordination {CuO$_x$} environments are rare[74] in the literature, but the related non-fluorinated complex,[Cu(O^{t}Bu)$_2$]$^-$, was also determined to have a linear two-coordinate geometry.[75-78] No details of its reactivity with O$_2$ were reported.

In order to explore the influence of phosphine steric bulk on Cu alkoxide geometries, the [(R$_3$P)Cu(μ-OR)$_2$Cu(PR$_3$)] series was synthesized through combination of PPh$_3$ and HOR with {Cu^I(mes)}$_n$ (Scheme 6), with bridging ligand OR= OC$_6$F$_5$ (**8**), OC$_4$F$_9$ (**9**), or OCPhMe$^F_2$ (**10**). When Pcy$_3$ was substituted for PPh$_3$ with the OR=OC$_4$F$_9$, steric bulk prevented formation of a dimer and instead resulted in linear [(cy$_3$P)Cu(OC$_4$F$_9$)] (**11**).[62] Complexes **8-10** are three-coordinate at Cu with a butterfly-type {Cu$_2$O$_2$} rhombus whose fold angle in the solid state is dependent on the identity of OR, with **8** having a planar {Cu$_2$O$_2$} rhombus, **10** being slightly bent, and **9** having the sharpest fold of 128.41(9)°. Fold angles were found to be dependent on the orbital interactions between Cu and O.[62] Compound **9** was also found to have a Cu…Cu distance of 2.8315(5)Å, consistent with a metallophilic interaction, as a result of the fold angle.[62]

Most recently, K[(R$_3$P)Cu(pin^F)] complexes were synthesized in order to explore the effect of a more stabilizing bidentate ligand.[63] We employed our expertise with KHpin^F as the ligand source in combination with Cu(I) (Scheme 6). A phosphine source was added to stabilize the coordination sphere, PPh$_3$ (**12**) or Pcy$_3$ (**13**). These complexes were prepared with both free K$^+$ (**12-13**), and with K$^+$ encapsulated with 18C6 (**14-15**). X-ray crystallography of **12** revealed a distorted trigonal-planar geometry, with three K···F/O interactions. Complexes **13-15**, which were not characterized by X-ray crystallography, are proposed to have anions structurally similar to
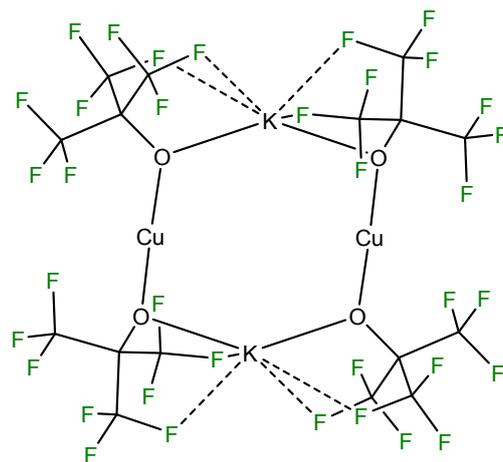
Scheme 7. Schematic diagram of **1** showing intramolecular K···F interactions as dotted lines.

12.[63] Compared to monodentate **1**, bidentate **12** has significantly fewer K···F/O interactions in the solid state, likely due to the presence of PPh$_3$.[61, 63]
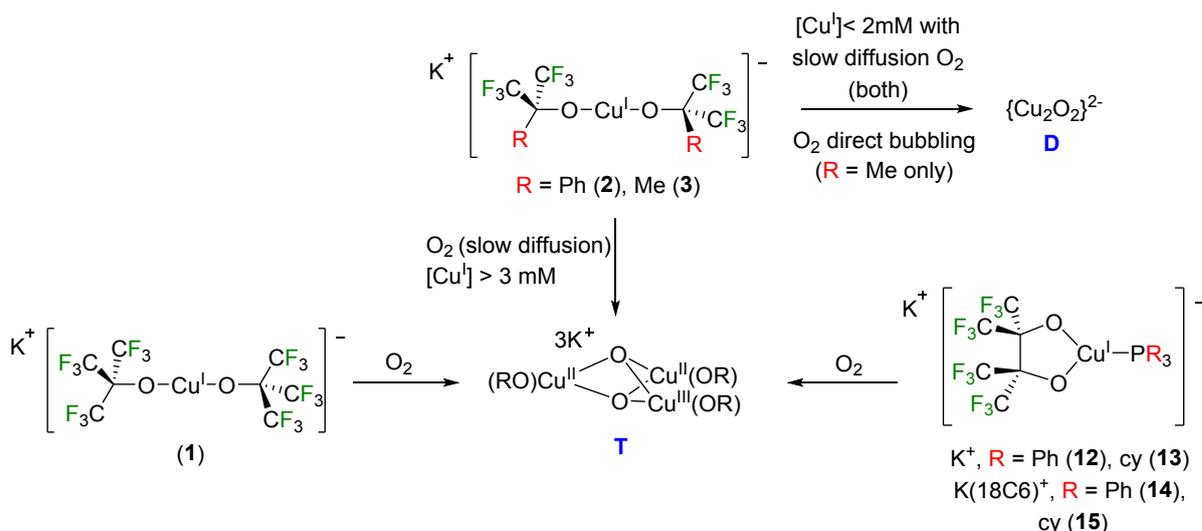
Scheme 8. Known reactivity of Cu(I) alkoxides with O_2.

The solution conductivity of **1-6** revealed the degree of ionic character of these complexes in solutions. As expected, **4-7** behaved as 1:1 electrolytes, indicating an ionic solution, with fully dissociated cations and anions. Unexpectedly, **1-3** showed significantly decreased conductivity compared to the complexes with encapsulated $[K(18C6)]^+$, indicating that more K···F/O interactions, shown in Scheme 7, result in compounds that do not fully dissociate in solution. Dimeric $[(Ph_3P)Cu(\mu-OR)_2Cu(PPh_3)]$ **8-10** showed no ionic species present in solution, demonstrating that the dimers are robust and do not exist in equilibrium with a charged form, such as $[(R_3P)_2Cu][Cu(OR)_2]$.[62, 79]

Reduction of O_2 and Intermediate Stoichiometries

Both the monodentate $K[Cu(OR)_2]$ and bidentate $K[(R_3P)Cu(pin^F)]$ complex families were tested for reactivity with O_2. Addition of O_2 to a solution of fully fluorinated **1**, with the monodentate OC_4F_9 ligand, led to the formation of a deep purple intermediate which was then evaluated by manometry and shown to form in a 3:1 Cu:O_2 ratio at all concentrations; this intermediate was postulated to be a trinuclear species, $\{Cu_3(\mu_3-O)_2\}^{3-}$, $\mathbf{T_{OC4F9}}$ (Scheme 8).[61] This structure was confirmed by cryospray-ionization mass spectrometry (CSI-MS). Notably, $\mathbf{T_{OC4F9}}$ is the first O-donor **T** core to be characterized by resonance Raman spectroscopy, with O···O vector stretches at 718 (^{16}O) and 671 cm^{-1} (^{18}O). These assignments were confirmed by DFT analysis.[80] Both **2** and **3** on the other hand, with partially fluorinated monodentate ligands, show concentration dependent reactivity with O_2. When $[Cu^I]$ > 3 mM and O_2 is introduced via slow diffusion, **2** affords a dark blue solution, and **3** afforded a dark red-brown. A 3:1 stoichiometry is observed by manometry at these concentrations, indicating formation of $\mathbf{T_{OCPhMeF2}}$ for **2** and $\mathbf{T_{OCMeMeF2}}$ for **3**.[61]

When $[Cu^I]$ < 2 mM, the resulting spectrum of **2** is red-shifted from λ= 496 and 590 nm to 644 nm. For **3**, similar shifts were observed.[61] In these cases, manometry indicated a 2:1 Cu:O_2 stoichiometry, corresponding to dimers $\mathbf{D_{OCPhMeF2}}$ and $\mathbf{D_{OCMeMeF2}}$. There are two possible electronic structures for such dimers, $\{Cu(III)(\mu-O_2)_2Cu(III)\}$,

O, and $\{Cu(II)(\eta^2,\eta^2-O_2)Cu(II)\}$, ^{S}**P**, which can exist in equilibrium with one another, depending on the solvent (Scheme 9).[81] The electronic spectra of $\mathbf{D_{OCPhMeF2}}$ and $\mathbf{D_{OCMeMeF2}}$ are most consistent with a $\{Cu(III)(\mu-O_2)_2Cu(III)\}$ core, based on the N-donor ligand literature,[13-15] but confirming vibrational data have not been obtained. $\mathbf{D_{OCMeMeF2}}$ was determined to have low stability in solution, starting to decay immediately following full formation. The long-term stability of $\mathbf{D_{OCPhMeF2}}$ was not evaluated.

Formation of $\mathbf{T_{OCMeMeF2}}$ was also shown to be dependent on the rate of O_2 addition, as noted in Scheme 8. Directly bubbling O_2 into a solution of **3** at all Cu(I) concentrations results in formation of the dimer. Similarly, directly bubbling O_2 into a solution of fully formed $\mathbf{T_{OCMeMeF2}}$ results in conversion to the dimer $\mathbf{D_{OCMeMeF2}}$.[61] These different results based on method of O_2 addition demonstrate our control over forming dimer or trimer, based on ligand and Cu:O_2 ratio. This behavior was not observed for $\mathbf{T_{OC4F9}}$.

Complexes **4** and **7** were also examined for O_2 reactivity; however, both showed no color change upon addition of O_2 under identical low temperature conditions.[61] It was hypothesized that fewer K···F/O interactions result in diminished ability to generate a stable $\{Cu_n-O_2\}$ species in this complex series.

Evaluation of complexes **12-15** for O_2 reactivity allowed for a comparison of how the presence of two monodentate versus one bidentate ligand affects Cu(I) reactivity. When **12-15** were exposed to O_2, a teal species formed.[63] UV-Vis spectra of all four species exhibited similar electronic transitions and extinction coefficients, and therefore are proposed to have the same core structure. To date, only reactivity with **12** has been extensively characterized. CSI-MS showed the stoichiometry of the reactive Cu-O_2 species of **12** to be $\{Cu_3(\mu_3-O)_2\}^{3-}$, $\mathbf{T_{pinF}}$, identical to $\mathbf{T_{OC4F9}}$ core (Scheme 9). Additionally, $\mathbf{T_{pinF}}$ was evaluated by EPR at -196 °C, showing a triplet ground state core that is consistent with other characterized **T** systems.[63, 82, 83] Because all four $[(R_3P)Cu(pin^F)]^-$ species have similar reactivity with

O_2, we deduce that K···F/O interactions do not strongly influence these complexes' abilities to reduce O_2.

These polynuclear $\{Cu_nO_2\}$ species have measurable lifetimes at lower temperatures, but none are significantly stable above -40 °C. T_{OC4F9} is stable at -80 °C for at least three hours.[80] Both $T_{OCMeMeF2}$ and $T_{OCPhMeF2}$ are stable at -80 °C for at least one hour,[61] and T_{pinF} for at least 30 minutes.[63] Formation of **T** for all ligand scaffolds is irreversible either from vacuum or bubbling N_2.
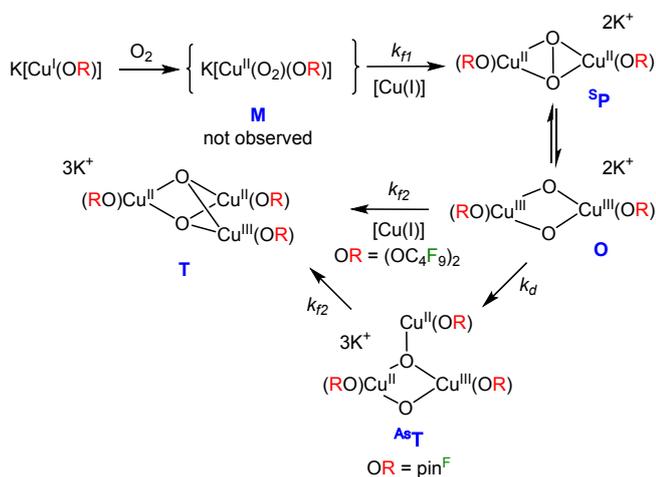
Scheme 9. Formation of $\{Cu_3O_2\}^{3-}$ species T_{pinF} and T_{OC4F9} upon reaction with O_2.

Because T_{OC4F9} and T_{pinF} have the same core structure, their mechanisms of formation were investigated in detail via a stopped-flow spectroscopy kinetic study (Scheme 9). As expected, both Cu(I) complexes interact with O_2 in a step-wise fashion. When bidentate **12** is mixed with O_2 in the stopped-flow reaction, a species with λ= 380 and 480 nm forms in the first five seconds and then rapidly decays. This species is proposed to have a $\{Cu(III)(\mu\text{-}O_2)_2Cu(III)\}$ core, O_{pinF}, based on the UV-Vis data (vide infra), and has a $k_{f1} = 0.418(1)$ s^{-1}. O_{pinF} transitions decay, with $k_d = 0.049(1)$ s^{-1}, giving way to formation of T_{pinF}. However, the k_{f2} of T_{pinF} is 0.268(6) s^{-1}, indicating that an intermediate must exist. DFT calculations have identified this as an asymmetric trimer, ^{As}T, as the likely intermediate.[63] We propose that a mononuclear $\{Cu\text{-}O_2\}$ species, **M**, must be formed initially; however, no kinetically resolvable chromophore is observed within the time limitations of the spectrometer.

T_{OC4F9} obtained from **1** has a similar formation pathway, but no observable intermediates between a dinuclear species and the final, symmetric trimer were indicated by the kinetic data. The two *d-d* transitions of deep purple T_{OC4F9} slowly grow in over 25 minutes. Fitting of single-wavelength data led us to detect two discrete steps: $\{Cu_2O_2\}$ (D_{OC4F9}) growth with $k_{f1} = 0.96(5)$ s^{-1}, and conversion of D_{OC4F9} into the trimer with $k_{f2} = 0.009(3)$ s^{-1}.[80] Interestingly, D_{OC4F9} forms more quickly compared to O_{pinF}, possibly due to the more flexible monodentate OC_4F_9 ligands, which may also explain why (to date) conditions for spectroscopic isolation of D_{OC4F9} have not been found. In contrast, T_{OC4F9} has a much slower rate of formation from D_{OC4F9} than that of T_{pinF} from O_{pinF}. This difference could arise because the bidentate ligands are closer to their final configuration in O_{pinF} versus

those in D_{OC4F9}. These observations reveal that while the different fluorinated O-donor ligands do not affect the identity of the final Cu_n-O_2 core, the ligand coordination does affect the rate of **T** formation. The formation of $^{As}T_{pinF}$ en route to $^{Sy}T_{pinF}$, may also be due to the decreased flexibility of the chelating ligand. For the monodentate series only, **1 – 3**, the K···F/O interactions are required for formation of a low-temperature stable Cu_n-O_2 intermediate.

Reactivity of $\{Cu_3$-$O_2\}$ with Substrates

Reactive $\{M_n$-$O_x\}$ species can have either nucleophilic or electrophilic character at the O atom. Both types of reactivity were seen in these systems. Using the relatively stable $T_{OCMeMeF2}$, $T_{OCPhMeMeF2}$, T_{OC4F9}, and T_{pinF} $\{Cu_3O_2\}$ cores, nucleophilic reactivity with CO_2 and oxidase/oxygenase reactivity with C-H bonds were probed. The oxidation reactions are summarized in Scheme 10. It should be noted that in the formation of T_{pinF}, all PR_3 is oxidized to OPR_3, with a ^1H NMR yield of 88% per $\{Cu_3O_2\}$.[63]

$T_{OCMeMeF2}$, $T_{OCPhMeMeF2}$, and T_{OC4F9} were evaluated for nucleophilic reactivity with CO_2.[61] Exposure to CO_2 led to color change upon warming, and the T_{OC4F9} or $T_{OCPhMeMeF2}$ cases yielded powders that when analyzed by IR spectroscopy indicated the presence of bound CO_3^{2-}, but no clean products were able to be isolated. Reaction of CO_2 and $T_{OCMeMeF2}$ yielded blue crystals of a Cu(II) alkoxide carbonate tetramer, $\{\{K_2(DME)_{1.5}\}[Cu(OCMeMe^F_2)_2(CO_3)]\}_4$, along with an unidentified green species.[61]

The partially fluorinated $T_{OCMeMeF2}$ and $T_{OCPhMeMeF2}$ species were found to perform intramolecular ligand hydroxylation. The $\{Cu_3O_2\}$ species were generated at -80 °C and then allowed to warm to room temperature, upon which a color shift to green was observed. These solutions were analyzed by ESI-MS, and the hydroxylated free ligands were identified. This analysis was repeated with isotopically labeled ^{18}O, resulting in a mixture of labeled and unlabeled free ligand, confirming O_2 as the source of the oxygen in intramolecular ligand hydroxylation.[61] These two **T** cores highlight the advantage of full ligand fluorination of T_{OC4F9} and T_{pinF} which are inherently immune to C-H oxidation and can direct their oxidation chemistry to external substrates.
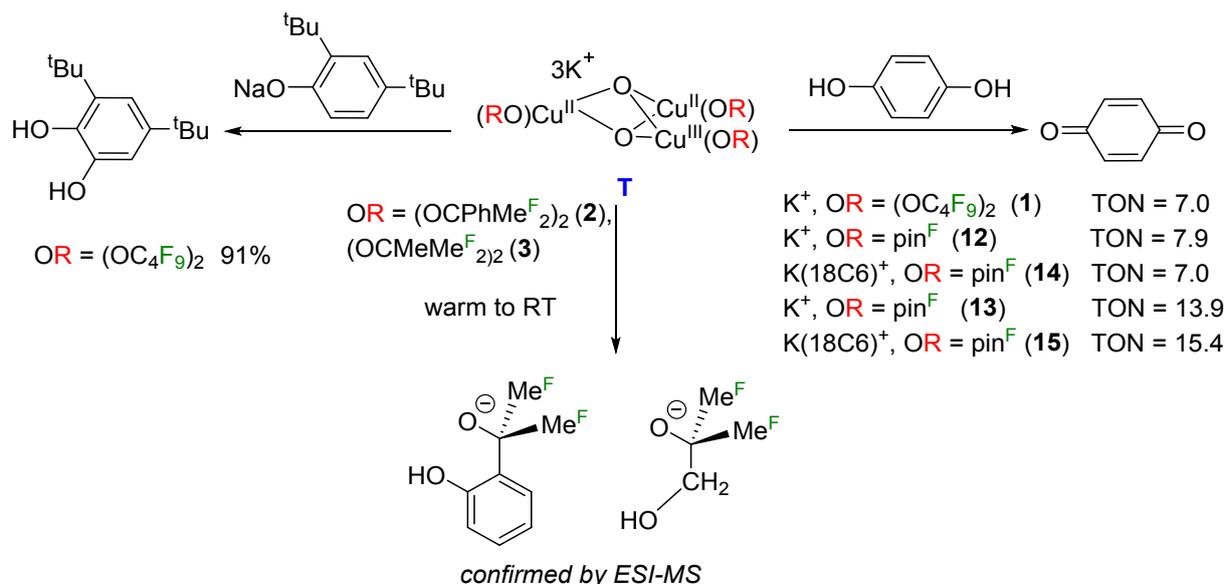
Scheme 10. Oxidation reactivity of O-donor **T** cores.

Oxidase reactivity was probed in the conversion of *para*-hydroquinone (H_2Q) to *para*-benzoquinone (BQ) (Scheme 10). Catalytic oxidation with **T$_{pinF}$** was observed with modest turnover. Notably, the identity of phosphine has a measurable effect on TON, whereas encapsulation of K^+ has little effect (**12** vs **14**). Total recovery of H_2Q and BQ is 94%, indicating clean reactivity.[63] **T$_{OC4F9}$** was also shown to catalytically convert H_2Q to BQ, with a comparable TON (**12**, **14** vs **13**, **15**) . Product recovery is lower, however, at 48%.[80] Similar TONs for these two trimers suggest that oxidase reactivity is not affected by ligand coordination environment of the {Cu$_3$O$_2$}$^{3-}$ unit., The rigidity of the pin^F ligand likely results in more **T** stability during oxidase reactivity. This effect may also lead less side reactivity as indicated by higher recovery of unreacted H_2Q.

Intermolecular monooxygenase reactivity was also investigated for both **T$_{OC4F9}$** and **T$_{pinF}$**. Excitingly, **T$_{OC4F9}$** was shown to be able to stoichiometrically hydroxylate 2,4-di-tert-butylphenolate (DBP) to 3,5-di-tert-butylcatecholate (DBC) (Scheme 10). The typical product observed is the *ortho*-substituted DBC; however, 10% of reactions resulted in small amounts of the *meta*-substituted DBC. Again O$_2$ was confirmed as the source of the oxygen atoms by an isotopic labeling experiment with $^{18}O_2$.[80] This system is not only the first O-donor **T** core to exhibit this reactivity, but also the first symmetric {Cu$_3$O$_2$} system to perform hydroxylation reactivity. Other trimeric Cu-O$_2$ species have been shown to do substrate hydroxylation,[51-53, 84] but not with a symmetric **T** core structure. Notably, **T$_{pinF}$** had no reactivity with DBP. Phenolates with other substituents were explored, however, no oxidase or oxygenase reactivity was observed with these substrates for either trimer, and **T$_{OC4F9}$** was found incapable of catalytic oxidation of DBP.[80] **T$_{OC4F9}$** and **T$_{pinF}$** were both also found not to abstract hydrogen atoms from 9,10-dihydroanthracene.[63, 80] These results further show that ligand environment influences hydroxylation capabilities of {Cu$_3$O$_2$}$^{3-}$ cores. The greater flexibility of the

monodentate ligands of **T$_{OC4F9}$** may provide a more accessible site for hydroxylation to occur, which cannot occur in the more rigid ligand environment of **T$_{pinF}$**.

Conclusions and Future Directions

Cu(I) complexes with mono- and bidentate fluorinated alkoxides react rapidly with O$_2$ to form {Cu$_3$O$_2$} cores that can effect intra- and intermolecular hydroxylation of sp^2- and sp^3-hybridized C-H bonds as well as one example of carbonate formation from CO$_2$. Three different factors have been considered: cation encapsulation, ligand coordination (monodentate vs bidentate), and presence of phosphine.

Potassium encapsulation was shown to affect **T** formation in the monodentate series, but not in the bidentate complexes. Due to the quantitative and qualitative differences in K···F/O interactions affecting Cu-O$_2$ reactivity, further investigation of the effect of the nature of the cation (K^+ vs Na$^+$ or Cs$^+$) and its encapsulation is ongoing. Greater exploration of cation···F/O interactions are also underway in a Sn-containing system, including by variable temperature ^{19}F NMR.[85]

Both the intra- and intermolecular reactivity of **T** intermediates were shown to be dependent on ligand identity and coordination. Ligand flexibility partially determined whether hydroxylation could be performed, as the monodentate complexes were more reactive. In particular, partially hydrogenated **T$_{OCMeMeF2}$** and **T$_{OCPhMeF2}$** underwent intramolecular ligand hydroxylation, whereas their fully fluorinated counter-part, **T$_{OC4F9}$**, was found to perform phenolic hydroxylation in addition to oxidase catalysis. The more rigid **T$_{pinF}$**, on the other hand, only effected hydroquinone oxidation and was unable to perform hydroxylation reactions, but the **T$_{pinF}$** chromophore persists at higher temperatures than for **T$_{OC4F9}$**. The mechanisms of the oxidation reactions will also be investigated in more detail. Preliminary data

suggest that proton and electron transfer steps are involved, rather than H atom abstraction.

Phosphine served to complete the coordination sphere for the bidentate complexes. Interestingly, in contrast to the monodentate species, all four compounds formed visible **T** species, regardless of cation encapsulation. In the pin^F series, the starting material with Pcy$_3$ led to double the TON versus that with PPh$_3$. Similarly, future studies on the formation of **T$_{pinF}$** from K[(cy$_3$P)Cu(pin^F)] could show how the different phosphines effect formation of **T**. Going forward, it is interesting to consider how [(R$_3$P)Cu(μ-OR)$_2$Cu(PR$_3$)] complexes would behave. As this series is deficient in alkoxide and contains coordinated PPh$_3$, this may result in different O$_2$ activation {Cu$_n$O$_2$} moieties. Continued exploration into Cu(I) O-donor complexes will reveal a greater understanding of how the coordination environment affects Cu-O$_2$ oxidation chemistry.

Conflicts of interest

There are no conflicts to declare.

Acknowledgements

Notes and references

1. M. Rolff, J. Schottenheim, H. Decker and F. Tuczek, *Chem. Soc. Rev.*, 2011, **40**, 4077-4098.
2. R. A. Steiner, K. H. Kalk and B. W. Dijkstra, *Proc. Natl. Acad. Sci. USA*, 2002, **99**, 16625-16630.
3. R. L. Peterson, S. Kim and K. D. Karlin, in *Comprehensive Inorganic Chemistry II (Second Edition)*, ed. K. Poeppelmeier, Elsevier, Amsterdam, 2013, DOI: https://doi.org/10.1016/B978-0-08-097774-4.00309-0, pp. 149-177.
4. W. Keown, J. B. Gary and T. D. P. Stack, *J. Biol. Inorg. Chem.*, 2017, **22**, 289-305.
5. M. Reglier, C. Jorand and B. Waegell, *J. Chem. Soc., Chem. Commun.*, 1990, 1752-1755.
6. C. Citek, S. Herres-Pawlis and T. D. P. Stack, *Acc. Chem. Res.*, 2015, **48**, 2424-2433.
7. Z. Huang, M. S. Askari, K. V. N. Esguerra, T.-Y. Dai, O. Kwon, X. Ottenwaelder and J.-P. Lumb, *Chem. Sci.*, 2016, **7**, 358-369.
8. P. Liebhäuser, K. Keisers, A. Hoffmann, T. Schnappinger, I. Sommer, A. Thoma, C. Wilfer, R. Schoch, K. Stührenberg, M. Bauer, M. Dürr, I. Ivanović-Burmazović and S. Herres-Pawlis, *Chem. Eur. J.*, 2017, **23**, 12171-12183.
9. E. L. Presti, E. Monzani, L. Santagostini and L. Casella, *Inorg. Chim. Acta*, 2018, **481**, 47-55.
10. B. Herzigkeit, B. M. Flöser, T. A. Engesser, C. Näther and F. Tuczek, *Eur. J. Inorg. Chem.*, 2018, **2018**, 3058-3069.
11. B. Herzigkeit, B. M. Flöser, N. E. Meißner, T. A. Engesser and F. Tuczek, *ChemCatChem*, 2018, **10**, 5402-5405.
12. K. V. N. Esguerra, Y. Fall and J.-P. Lumb, *Inorg. Chim. Acta*, 2018, **481**, 197-200.
13. L. M. Mirica, X. Ottenwaelder and T. D. P. Stack, *Chem. Rev.*, 2004, **104**, 1013-1045.
14. E. A. Lewis and W. B. Tolman, *Chem. Rev.*, 2004, **104**, 1047-1076.
15. C. E. Elwell, N. L. Gagnon, B. D. Neisen, D. Dhar, A. D. Spaeth, G. M. Yee and W. B. Tolman, *Chem. Rev.*, 2017, **117**, 2059-2107.
16. B. E. R. Snyder, M. L. Bols, R. A. Schoonheydt, B. F. Sels and E. I. Solomon, *Chem. Rev.*, 2018, **118**, 2718-2768.
17. W. Vermeiren and J.-P. Gilson, *Top. Catal.*, 2009, **52**, 1131-1161.
18. P. Vanelderen, B. E. R. Snyder, M.-L. Tsai, R. G. Hadt, J. Vancauwenbergh, O. Coussens, R. A. Schoonheydt, B. F. Sels and E. I. Solomon, *J. Am. Chem. Soc.*, 2015, **137**, 6383-6392.
19. G. I. Pannov, V. I. Sobolev and A. S. Kharitonov, *J. Mol. Catal.*, 1990, **61**, 85-97.
20. M. H. Groothaert, P. J. Smeets, B. F. Sels, P. A. Jacobs and R. A. Schoonheydt, *J. Am. Chem. Soc.*, 2005, **127**, 1394-1395.
21. P. J. Smeets, R. G. Hadt, J. S. Woertink, P. Vanelderen, R. A. Schoonheydt, B. F. Sels and E. I. Solomon, *J. Am. Chem. Soc.*, 2010, **132**, 14736-14738.
22. J. S. Woertink, P. J. Smeets, M. H. Groothaert, M. A. Vance, B. F. Sels, R. A. Schoonheydt and E. I. Solomon, *Proc. Natl. Acad. Sci. USA*, 2009, **106**, 18908-18913.
23. G. Li, P. Vassilev, M. Sanchez-Sanchez, J. A. Lercher, E. J. M. Hensen and E. A. Pidko, *J. Catal.*, 2016, **338**, 305-312.
24. M. A. C. Markovits, A. Jentys, M. Tromp, M. Sanchez-Sanchez and J. A. Lercher, *Top. Catal.*, 2016, **59**, 1554-1563.
25. S. Grundner, M. A. C. Markovits, G. Li, M. Tromp, E. A. Pidko, E. J. M. Hensen, A. Jentys, M. Sanchez-Sanchez and J. A. Lercher, *Nat. Comm.*, 2015, **6**, 7546.
26. D. C. Bradley, R. C. Mehrotra, I. P. Rothwell and A. Singh, *Alkoxo and Aryloxo Derivatives of Metals*, Academic Press, San Diego, California, USA, 2001.
27. A. Bell-Taylor, J. D. Gorden, E. E. Hardy and C. R. Goldsmith, *Inorg. Chim. Acta*, 2018, **482**, 206-212.
28. Y. M. Kim, K.-B. Cho, J. Cho, B. Wang, C. Li, S. Shaik and W. Nam, *J. Am. Chem. Soc.*, 2013, **135**, 8838-8841.
29. S. N. Dhuri, K.-B. Cho, Y.-M. Lee, S. Y. Shin, J. H. Kim, D. Mandal, S. Shaik and W. Nam, *J. Am. Chem. Soc.*, 2015, **137**, 8623-8632.
30. S. Riedel and M. Kaupp, *Coord. Chem. Rev.*, 2009, **253**, 606-624.
31. C. J. Willis, *Coord. Chem. Rev.*, 1988, **88**, 133-202.
32. M. C. Buzzeo, A. H. Iqbal, C. M. Long, D. Millar, S. Patel, M. A. Pellow, S. A. Saddoughi, A. L. Smenton, J. F. C. Turner, J. D. Wadhawan, R. G. Compton, J. A. Golen, A. L. Rheingold and L. H. Doerrer, *Inorg. Chem.*, 2004, **43**, 7709-7725.
33. A. P. Purdy, C. F. George and G. A. Brewer, *Inorg. Chem.*, 1992, **31**, 2633-2638.
34. S.-C. Roşca, T. Roisnel, V. Dorcet, J.-F. Carpentier and Y. Sarazin, *Organometallics*, 2014, **33**, 5630-5642.
35. S. M. Balasekaran, A. Hagenbach, M. Drees and U. Abram, *Dalton Trans.*, 2017, **46**, 13544-13552.

36. S. Bulut, P. Klose and I. Krossing, *Dalton Trans.*, 2011, **40**, 8114-8124.

37. T. S. Cameron, G. B. Nikiforov, J. Passmore and J. M. Rautiainen, *Dalton Trans.*, 2010, **39**, 2587-2596.

38. S. M. Ivanova, B. G. Nolan, Y. Kobayashi, S. M. Miller, O. P. Anderson and S. H. Strauss, *Chem. Eur. J.*, 2001, **7**, 503-510.

39. M. E. Pascualini, S. A. Stoian, A. Ozarowski, N. V. Di Russo, A. E. Thuijs, K. A. Abboud, G. Christou and A. S. Veige, *Dalton Trans.*, 2015, **44**, 20207-20215.

40. D. Zeng, M. Ren, S.-S. Bao and L.-M. Zheng, *Inorg. Chem.*, 2014, **53**, 795-801.

41. S. F. Hannigan, J. S. Lum, J. W. Bacon, C. Moore, J. A. Golen, A. L. Rheingold and L. H. Doerrer, *Organometallics*, 2013, **32**, 3429-3436.

42. J. L. Steele, L. Tahsini, C. Sun, J. K. Elinburg, C. M. Kotyk, J. McNeely, S. A. Stoian, A. Dragulescu-Andrasi, A. Ozarowski, M. Ozerov, J. Krzystek, J. Telser, J. W. Bacon, J. A. Golen, A. L. Rheingold and L. H. Doerrer, *Chem. Commun.*, 2018, **54**, 12045-12048.

43. S. A. Cantalupo, S. R. Fiedler, M. P. Shores, A. L. Rheingold and L. H. Doerrer, *Angew. Chem., Int. Ed.*, 2012, **51**, 1000-1005.

44. B. N. Zheng, M. O. Miranda, A. G. Di Pasquale, J. A. Golen, A. L. Rheingold and L. H. Doerrer, *Inorg. Chem.*, 2009, **48**, 4274-4276.

45. J. S. Lum, P. E. Chen, A. L. Rheingold and L. H. Doerrer, *Polyhedron*, 2013, **58**, 218-228.

46. S. A. Cantalupo, H. E. Ferreira, E. Bataineh, A. J. King, M. V. Petersen, T. Wojtasiewicz, A. G. DiPasquale, A. L. Rheingold and L. H. Doerrer, *Inorg. Chem.*, 2011, **50**, 6584-6596.

47. S. A. Cantalupo, J. S. Lum, M. C. Buzzeo, C. Moore, A. G. Di Pasquale, A. L. Rheingold and L. H. Doerrer, *Dalton Trans.*, 2010, **39**, 374-383.

48. M. Allan and C. J. Willis, *J. Am. Chem. Soc.*, 1968, **90**, 5343-5344.

49. L. Tahsini, S. E. Specht, J. S. Lum, J. J. M. Nelson, A. F. Long, J. A. Golen, A. L. Rheingold and L. H. Doerrer, *Inorg. Chem.*, 2013, **52**, 14050-14063.

50. B. A. Jazdzewski, A. M. Reynolds, P. L. Holland, V. G. Young, S. Kaderli, A. D. Zuberbühler and W. B. Tolman, *J. Biol. Inorg. Chem.*, 2003, **8**, 381-393.

51. S. I. Chan, Y.-J. Lu, P. Nagababu, S. Maji, M.-C. Hung, M. M. Lee, I.-J. Hsu, P. D. Minh, J. C.-H. Lai, K. Y. Ng, S. Ramalingam, S. S.-F. Yu and M. K. Chan, *Angew. Chem. Int. Ed.*, 2013, **52**, 3731-3735.

52. S. Maji, J. C.-M. Lee, Y.-J. Lu, C.-L. Chen, M.-C. Hung, P. P.-Y. Chen, S. S.-F. Yu and S. I. Chan, *Chem. Eur. J.*, 2012, **18**, 3955-3968.

53. P. P.-Y. Chen, R. B.-G. Yang, J. C.-M. Lee and S. I. Chan, *Proc. Natl. Acad. Sci. USA*, 2007, **104**, 14570-14575.

54. M. S. Nasir, K. D. Karlin, D. McGowty and J. Zubieta, *J. Am. Chem. Soc.*, 1991, **113**, 698-700.

55. K. D. Karlin, P. Ghosh, R. W. Cruse, A. Farooq, Y. Gultneh, R. R. Jacobson, N. J. Blackburn, R. W. Strange and J. Zubieta, *J. Am. Chem. Soc.*, 1988, **110**, 6769-6780.

56. I. López, R. Cao, D. A. Quist, K. D. Karlin and N. Le Poul, *Chem. Eur. J.*, 2017, **23**, 18314-18319.

57. N. N. Murthy, M. Mahroof-Tahir and K. D. Karlin, *Inorg. Chem.*, 2001, **40**, 628-635.

58. F. Gennarini, R. David, I. López, Y. Le Mest, M. Réglier, C. Belle, A. Thibon-Pourret, H. Jamet and N. Le Poul, *Inorg. Chem.*, 2017, **56**, 7707-7719.

59. R. Cao, L. T. Elrod, R. L. Lehane, E. Kim and K. D. Karlin, *J. Am. Chem. Soc.*, 2016, **138**, 16148-16158.

60. R. Cao, C. Saracini, J. W. Ginsbach, M. T. Kieber-Emmons, M. A. Siegler, E. I. Solomon, S. Fukuzumi and K. D. Karlin, *J. Am. Chem. Soc.*, 2016, **138**, 7055-7066.

61. J. S. Lum, L. Tahsini, J. A. Golen, C. Moore, A. L. Rheingold and L. H. Doerrer, *Chem. Eur. J.*, 2013, **19**, 6374-6384.

62. P. E. Chen, J. McNeely, J. S. Lum, E. J. Gardner, V. Phillips, J. A. Golen, A. L. Rheingold and L. H. Doerrer, *Polyhedron*, 2016, **116**, 204-215.

63. S. F. Hannigan, A. I. Arnoff, S. E. Neville, J. S. Lum, J. A. Golen, A. L. Rheingold, N. Orth, I. Ivanović-Burmazović, P. Liebhäuser, T. Rösener, J. Stanek, A. Hoffmann, S. Herres-Pawlis and L. H. Doerrer, *Chem. Eur. J.*, 2017, **23**, 8212-8224.

64. T. Tsuda, T. Yazawa, K. Watanabe, T. Fujii and T. Saegusa, *J. Org. Chem.*, 1981, **46**, 192-194.

65. M. Stollenz and F. Meyer, *Organometallics*, 2012, **31**, 7708-7727.

66. J. Nitsch, F. Lacemon, A. Lorbach, A. Eichhorn, F. Cisnetti and A. Steffen, *Chem. Commun.*, 2016, **52**, 2932-2935.

67. C. M. Lieberman, V. D. Vreshch, A. S. Filatov and E. V. Dikarev, *Inorg. Chim. Acta*, 2015, **424**, 156-161.

68. D. Yadav, R. Kumar Siwatch, S. Sinhababu, S. Karwasara, D. Singh, G. Rajaraman and S. Nagendran, *Inorg. Chem.*, 2015, **54**, 11067-11076.

69. J. P. Fackler, *Inorg. Chim. Acta*, 2015, **424**, 83-90.

70. A. Bheemaraju, J. W. Beattie, Y. Danylyuk, J. Rochford and S. Groysman, *Eur. J. Inorg. Chem.*, 2014, **2014**, 5865-5873.

71. F. Schax, C. Limberg and C. Mügge, *Eur. J. Inorg. Chem.*, 2012, **2012**, 4661-4668.

72. T. C. Davenport and T. D. Tilley, *Angew. Chem. Int. Ed.*, 2011, **50**, 12205-12208.

73. M. A. Carvajal, S. Alvarez and J. J. Novoa, *Chem. Eur. J.*, 2004, **10**, 2117-2132.

74. P. Fiaschi, C. Floriani, M. Pasquali, A. Chiesi-Villa and C. Guastini, *Inorg. Chem.*, 1986, **25**, 462-469.

75. H. Yi, G. Zhang, J. Xin, Y. Deng, J. T. Miller, A. J. Kropf, E. E. Bunel, X. Qi, Y. Lan, J.-F. Lee and A. Lei, *Chem. Commun.*, 2016, **52**, 6914-6917.

76. G. Zhang, H. Yi, J. Xin, Y. Deng, R. Bai, Z. Huang, J. T. Miller, A. J. Kropf, E. E. Bunel, X. Qi, Y. Lan and A. Lei, *Org. Chem. Front.*, 2016, **3**, 975-978.

77. A. Zanardi, M. A. Novikov, E. Martin, J. Benet-Buchholz and V. V. Grushin, *J. Am. Chem. Soc.*, 2011, **133**, 20901-20913.

78. A. I. Konovalov, J. Benet-Buchholz, E. Martin and V. V. Grushin, *Angew. Chem. Int. Ed.*, 2013, **52**, 11637-11641.

79. J. W. Tye, Z. Weng, R. Giri and J. F. Hartwig, *Angew. Chem. Int. Ed.*, 2010, **49**, 2185-2189.

80. S. E. N. Brazeau, E. E. Norwine, S. F. Hannigan, N. Orth, I. Ivanovic-Burmazovic, D. Rukser, F. Biebl, B. Grimm-Lebsanft, G. Praedel, M. Teubner, M. Rubhausen, P. Liebhaeuser, T. Rosener, J. Stanek, A. Hoffmann, S. Herres-Pawlis and L. H. Doerrer, *Submitted*.

81. J. A. Halfen, S. Mahapatra, E. C. Wilkinson, S. Kaderli, V. G. Young, L. Que, A. D. Zuberbühler and W. B. Tolman, *Science*, 1996, **271**, 1397-1400.

82. T. E. Machonkin, P. Mukherjee, M. J. Henson, T. D. P. Stack and E. I. Solomon, *Inorg. Chim. Acta*, 2002, **341**, 39-44.
83. A. K. Gupta and W. B. Tolman, *Inorg. Chem.*, 2012, **51**, 1881-1888.
84. B. J. Cook, G. N. Di Francesco, M. T. Kieber-Emmons and L. J. Murray, *Inorg. Chem.*, 2018, **57**, 11361-11368.
85. J. K. Elinburg, T. M. Alam, S. Klenner, R. Pöttgen, A. L. Rheingold and L. H. Doerrer., *Manuscript in preparation*.